The effect of iron-particles on the electrical properties of n-GaSb semiconductor material

A Bele[1], LT Selepe[1], ME Sithole[1]

[1] Department of Physics, Sefako Makgatho Health Science University, P. O. Box 94, Medunsa, 0204, South Africa

E-mail address: abongile.bele@smu.ac.za

Abstract: Semiconductor material are characterized with the Schottky barrier diodes (SBDs) as a basic structure. The study was conducted in order to check the effect of iron (Fe^+) ions on the electrical properties of Gallium antimonide (n-GaSb) semiconductor material. GaSb was implanted with iron ions at various ion fluences ranging from 1.2×10^{15} ion.cm^{-2} to 1.2×10^{17} ions.cm^{-2} while keeping the ion energy at 90 keV. Aluminium (Al) SBDs were fabricated on the n-GaSb with Fe^+ at various fluences. Structural and electrical properties have been investigated using the Raman spectroscopy and I-V characterization, respectively. Raman spectroscopy showed a slight amorphization at fluences higher than 1.2×10^{15} ions.cm^{-2}. The ideality factor (n) increased from 1.3 for the un-implanted to 2.0 for 1.2×10^{17} ions.cm^{-2}. The barrier height was found to decrease from 0.74 eV for the non-implanted to 0.64 eV for 1.2×10^{17} ions.cm^{-2}. Generally, the barrier height decreased with the increasing implantation fluences while the ideality factor increased with the increasing doping fluences.

1. Introduction

Gallium antimonide have been used in a wide range of applications such as developing radiation detector diodes [1]. These semiconductor materials are also used for radiation detection in a nuclear reactor [2]. The other applications include the use in radio detectors, transistors, lasers and light emitting diodes. The elemental semiconductors have been preferred for the detection in X-ray and gamma-ray spectroscopy but were later faced with limitations because of their radiation intolerance [3]. The semiconductors usually improve their functioning if there are adequate impurities that are added on them [4]. The semiconductor materials can be grown at different temperature conditions but the highest growth temperature is 520 °C [5]. The electrical characteristics of the semiconductor materials differ especially when subjected to different temperature conditions. These characteristics also differ when different impurities are added on the semiconductor materials. It is important that we know what impurity material improve the electrical properties of the semiconductor materials.

The Schottky barrier height and the ideality factor that assumes the thermionic emission (TE) theory shows a strong dependence on temperature [6]. In the investigation of the effect caused by the annealing temperature to the electrical and structural properties of a fabricated W/p-lnP Schottky barrier diodes, it was found that these diodes exhibit the good rectification behaviour. The barrier height increases at 300 °C but decreases at 400 °C. The maximum barrier height is reached at 300 °C. The overall

surface morphology of the SBD does not change significantly at elevated temperatures [7]. The fabrication of Cp/p-type Si Schottky barrier diodes at various annealing temperatures from 200-600 °C shows that the barrier height fluctuates. It slightly decreases from 200-300 °C but it also increases from 400-600 °C [8]. During the study of Pd/ZnO Schottky barrier diodes with temperature, it was found that the ideality factor decreased with increasing temperature between 30-300 K while on the other hand the barrier height increased with increasing temperature [9].

The current-transport mechanism for the Au/Zn-doped PVA/n-GaAs Schottky barrier diodes shows that the ideality factor decreases while the Schottky barrier height increases for the investigated temperature dependency from 80-300 K [10]. The capacitance and conductance are strong functions of frequency and applied bias voltage. The conductance increases with increasing applied bias voltage while the capacitance decreases. The same happens with an increase in frequency [11]. The annealing temperature affect the electronic parameters and carrier transport mechanism of the Pt/n-type Ge Schottky diode. The diodes were annealed at temperatures between 183-303K and it was discovered that the zero-bias barrier height increased but the ideality factor decreased with increasing temperature [12]. The capacitance and conductance are strong functions of frequency and temperature. The capacitance and conductance for the Au/n-GaAs Schottky barrier diodes increases at low frequency [13]. The transport characteristics of Pd/epixial n-GaSb:Te Schottky barrier diodes were studied with current-voltage measurements between 80 and 300K. The barrier height and ideality factor apparently increased with decreasing temperature. SBDs have remarkable low and saturating reverse current-of the lowest ever reported for GaSb [14]. The Hall effect measurements show a decrease in carrier mobility as the hole concentration increases on a silicon doped GaSb. The study shows the decrease in inter-band gap energy of the semiconductor material. The thermal conductivities become very low due to a high thermal resistivity [15]. In the study, the electrical properties of the Fe^+ implanted n-GaSb were studied.

2. Experimental procedure

Fe^+ ions were implanted in the n-GaSb semiconductor samples using an ion implanter system. The Fe^+ implantation was conducted at different fluencies of 1.2×10^{15}, 1.2×10^{16} and 1.2×10^{17} ions.cm^{-2} at the energy of 90 keV. Raman spectra were measured by a Thermal micro-Raman system at room temperature for both non-implanted and implanted n-GaSb samples. The excitation was at 520 nm from a semiconductor diode laser. The electrical characterization of the SBDs fabricated on n-GaSb was performed by *I-V* at room temperature (300 K). The HP4141B pico Amp meter was used for *I-V* measurements. When measurements were performed, the voltage was varied from -0.5V to 0.5 V with the steps of 0.1 V. The *I-V* system measured the parameters including saturation current (Is), the ideality factor (*n*), the Schottky barrier height (Φ_b).

3. Results and Discussion

3.1. *Raman Spectroscopy*

Raman spectra of the un-implanted and the implanted GaSb samples at different fluencies of 1.2×10^{15}, 1.2×10^{16} and 1.2×10^{17} ions.cm^{-2} at the energy of 90 keV are discussed. Figure 1 shows the comparison of Raman spectra for un-implanted and Fe^+ implanted n-GaSb at different fluencies.
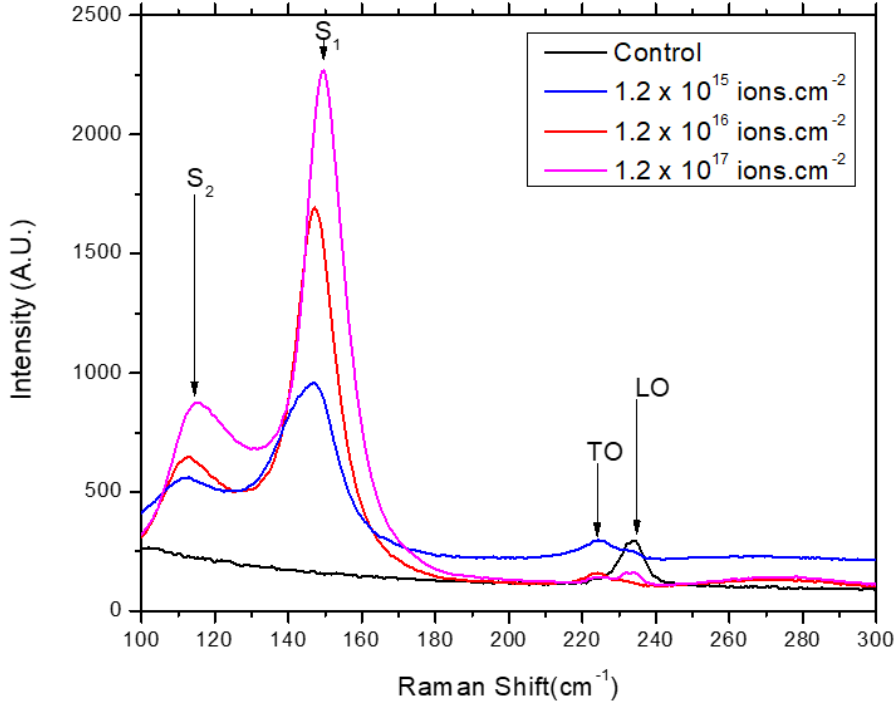
Figure 1. *Raman spectra for un-implanted and Fe$^+$ implanted n-GaSb at different fluences.*

The spectrum for the control sample shows a peak at 232.74 cm^{-1}. The peak correspond to the longitudinal optical (LO), which is an expected spectrum for the (100) plane [13]. In the sample implanted with 1.2×10^{15} Fe$^+$ ions.cm^{-2}, the LO phonons peak have been reduced and now a new peak emerges at 224.38 cm^{-1} which correspond to the Transverse optical (TO) phonons. In addition to the TO peak, new peaks were observed at 111.24 cm^{-1} (S$_1$) and 146.69 cm^{-1} (S$_2$). The reduction of LO phonons peak by ion implantation is associated with the disorder of crystalline structure of GaSb [16]. Nonetheless, the new peaks might be as a result of selective sputtering of Sb atoms during the ion implantation damage [17]. Regarding the sample implanted with 1.2×10^{16} Fe$^+$ ions.cm^{-2}, the LO phonons peak is not visible and the TO phonons peak is reduced and the new peaks are sharpening more. This might be due to ion implantation damage. For the sample implanted with 1.2×10^{16} Fe$^+$ ions.cm^{-2}, the LO phonons and TO phonons peaks have re-appeared but, however the new peaks are sharper. The comparison clearly illustrates the change in the structure of n-GaSb [16]. The change in the structure is due to the induced defects caused by Fe$^+$ ions. The GaSb is transformed into an amorphous state by Fe$^+$ implantation exceeding 1.2×10^{15} Fe$^+$ ions.cm^{-2}. This is also confirmed by [18].

3.2 I-V measurements

In this section, the *I-V* measurements of Al/n-GaSb Schottky barrier diodes (SBDs) at room temperature are presented. The current transport in the Schottky barrier diode is explained by majority carriers [6]. It may be described by thermionic emission (TE) mechanism over the interface barrier. The Schottky barrier height (ϕ_b) and the ideality factor (n) were determined by using the thermionic emission current voltage expression [19]:

$$I = I_s \left[\exp\left(\frac{q(V - IR_s)}{nkT} \right) - 1 \right].$$

(1)

where

$$I_s = AT^2 A^* \exp\left(\frac{-q\phi_b}{kT}\right),$$

(2)

where, R_s is the series resistance of the diode, V is the applied voltage, q is the electronic charge, k is the Boltzmann constant, T is the absolute temperature, A is the area of the diode. A^* is the effective Richardson constant, ϕ_b is the effective barrier height at zero bias and n is the ideality factor. A theoretical value of A^* used was 5.16 A cm^{-2} K^{-2} for GaSb [20]. The values of the ideality factor were derived from the following equation 3

$$n = \frac{q}{kT}\left(\frac{dV}{d(\ln I)}\right).$$

(3)

$$\phi_b = \frac{kT}{q}\ln\left(\frac{AA^*T^2}{I_s}\right).$$

(4)

ϕ_b was determined using equation 4 above.

Figure 2 shows the semi-log plot of the forward and reverse current as a function of applied voltage. The graphs represent Al/n-GaSb Schottky barrier diodes for the non-implanted and implanted samples with a fluences of 1.2×10^{15}, 1.2×10^{16} and 1.2×10^{17} Fe$^+$ ions.cm^{-2}.
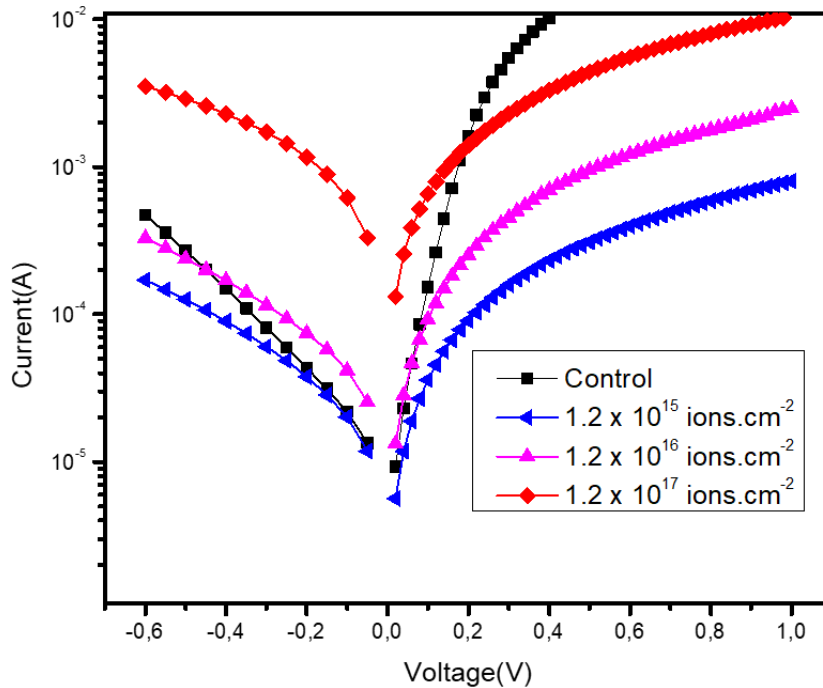

Figure 2: *The I-V characteristics of the un-implanted and implanted n-GaSb*

The as-deposited SBD showed good rectification properties which are attributed to the cleaning procedure used before deposition [21]. This curve shows two distinct linear regions as was also observed [21]. These regions are attributed by barrier height inhomogeneity; this is according to [9]. The Schottky barrier height evaluated on Al/n-GaSb was found to be 0.72 eV. This was higher than the 0.59 eV measured by [22], this might be due to the different material properties e.g. carrier concentration which is 10^{17}. The ideality factor was found to be 1.22 for the sample implanted with 1.2×10^{15} ion.cm^{-2}. The

ideality factor close to unity implies that the current transport is dominated by the thermionic emission mechanism [23]. It can be seen from the graphs that the gap between the forward and the reverse current decreases with an increase in the particle fluence. The curves deviate from linearity in the forward region which indicated that other current mechanisms contributes to the leakage current. These results show the evidence of generation-recombination current at low voltages and dominance of the thermionic emission at greater voltages [6]. Similar results were found by [24]. These SBDs are the same as the ones observed in Ge by [25]. The high ideality factor can be attributed to the surface damage by ion implantation.

The Schottky barrier height was observed to decrease with increasing the particle fluence, 0.73. 0.71 and 0,64 eV for particle fluence of 1.2×10^{15}, 1.2×10^{16} and 1.2×10^{17} ions/cm^2, respectively. The saturated current was increasing from 4.23×10^{-6} A to 1.05×10^{-4} A. The ideality factor decreased from 1.75 at 1.2×10^{15} to 1.64 at 1.2×10^{16} and then increased with the increasing particle fluence. This is consistent to the results that were found by [6].

4. Conclusion

This study was focused on the electrical properties of the n-GaSb semiconductor material. This semiconductor material was successfully implanted with Fe^+ ions at different ion fluencies while keeping the ion energy constant. These Fe^+ ions were implanted into the n-GaSb samples using a 350D ion implanter system. The Raman spectroscopy was used to check for the Raman activity. Raman spectroscopy showed that the material amorphized at fluences higher than 1.2×10^{15} ions.cm^{-2}. The aluminium Schottky contact as well as the gold-germanium ohmic contact have been successfully fabricated through electron beam deposition system on the front and the backsides of n-GaSb semiconductor material grown by LEC. All the samples including the implanted and non-implanted samples were analysed by *I-V* at room temperature. Generally, the barrier height decreased with the increasing implantation fluences while the ideality factor increased with the increasing implantation fluences.

References

[1]   Msimanga, M. McPherson, M. Theron C 2004 *Radiation Physics and Chemistry technology* **71** 2070-2073.
[2]   Holland AD, Short ADT, Cross T 1994 *Nuclear Instruments and Methods Section A* **346** 366-371.
[3]   Pitzl D, Cartiglia N, Hubbard B, Hutchinson D, Leslie J, O'Shaughnessy K, Rowe W, Sadrozinski HW, Seiden A, Spencer E, Ziock HJ, Ferguson P, Holzscheiter K, Sommer WF 1992 *Nuclear Instruments and Methods Section A* **311** 98-104.
[4]   Jones BK, Santana J, McPherson M 1997 *Nuclear Instruments* and *Methods Section A* **395** 81-87.
[5]   Keorperk E, Murray LM, Norton DT, Boggess TF, Prineas JP 2010 *Journal of Crystal Growth* **312** 185-191.
[6]   Huang WC, Lin TC, Horng CT, Lin YH 2013 *Materials science and semiconductor processing* **16** 418.
[7]   Reddy VR, Silpa DS, Hyung-Jong Y, Chel-Jong C 2014 *Superlattices and Microstructures* **71** 134-146.
[8]   Guler G, Karastas S, Bakkaloglu OF 2009 *Physics B: Condensed Matter* **404** 1494-1497.
[9]   Mayimele MA, Diale M, Mtangi W, Auret FD 2015 *Materials Science and Semiconductor Processing* **34** 359-364.

[10]   Teamer H, Turut A, Uslu H, Altindal S, Uslu I 2013 *Sensors and Actuators A: Physical* **199** 194-201.
[11]   Bilkan C, Gumus A, Altindal S 2015 *Materials Science and Semiconductor Processing* **39** 484-491.
[12]   Guo E, Zeng Z, Zhang Y, Leng X, Zhou H 2016 Wang X, *Microelectronics Reliability* 63-69.
[13]   Demirezen S, Ozavci E, Altindal S 2014 *Materials Science and Semiconductor Processing* **23** 1-6.
[14]   Venter A, Murape DM, Botha JR, Auret FD 2015 *Thin Solid Films* **574** 32-37.
[15]   Abroug S, Saadallah F, Genty F, Yacoubi N 2009 *Physics Procedia* **2** 787-795.
[16]   Jadhav V, Dubey SK, Dubey RL, Yadav AD. Kanjilal D 2009 *Surface and Coatings* **203** 2670-2673
[17]   Kim SG, Asahi H, Seta M, Takizawa J, Emura S, Soni RK, Gonda S, Tanoque H 1993 *Journal of Applied Physics* **74** 579.
[18]   Morehead Jr FF, Crowder BL 1970 *Radiat. Eff.* **6** 27
[19]   Rhoderick EH, Williams RH 1988 *Semiconductor Contacts*, 2nd ed. (Clarendon Press: Oxford).
[20]   Liu ZY, Saulys DA, Kuecha 2004 *Appl. Phys. Letter* **85** 1023-1033.
[21]   Ozavc E, Demirezen S, Aydemir U, Altndal S 2013 *Sensors and Actuators A: Physical* **194** 259-268.
[22]   Ramelan AH, Harjana, Pepen A, Goldys E 2010 *J Mater Dan Sains*. **15** 136.
[23]   Sze, SM 1998 *Physics of Semiconductor devices*, 1st ed. (New York: Wiley)
[24]   Chen JF, Chen NC, Liu HS 1996 *J. Electronic materials* **25** 1790-1800.
[25]   Coelho SMM, Auret FD, Janse van Rensburg PJ, Nele JM 2014 *Physica B: Condensed matter* **439** 97-100.